

RSC Advances



This is an *Accepted Manuscript*, which has been through the Royal Society of Chemistry peer review process and has been accepted for publication.

Accepted Manuscripts are published online shortly after acceptance, before technical editing, formatting and proof reading. Using this free service, authors can make their results available to the community, in citable form, before we publish the edited article. This *Accepted Manuscript* will be replaced by the edited, formatted and paginated article as soon as this is available.

You can find more information about *Accepted Manuscripts* in the [Information for Authors](#).

Please note that technical editing may introduce minor changes to the text and/or graphics, which may alter content. The journal's standard [Terms & Conditions](#) and the [Ethical guidelines](#) still apply. In no event shall the Royal Society of Chemistry be held responsible for any errors or omissions in this *Accepted Manuscript* or any consequences arising from the use of any information it contains.

Regioselective Synthesis of Vitamin K3 Based Dihydrobenzophenazine Derivative: Their Novel Crystal Structure and DFT Studies

Received 00th January 20xx,
Accepted 00th January 20xx

DOI: 10.1039/x0xx00000x

www.rsc.org/

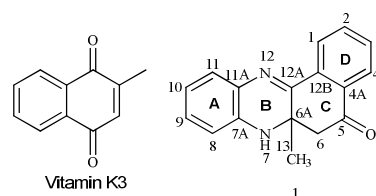
Dattatray Chadar^a, Soniya S. Rao^a, Shridhar P. Gejji^a, Bharat Ugale^b, C.M. Nagraja^b, Milind Nikalje^a and Sunita Salunke-Gawali^{a*}

A novel acid catalyzed regioselective Michael addition of *o*-phenylenediamine to VitaminK3 has been carried out to synthesize dihydrobenzophenazine derivative viz. 6a-methyl-6a,7-dihydrobenzo[α]phenazin-5(6H)-one (**1**). The compound has been characterized using the single crystal X-ray diffraction and density functional theory.

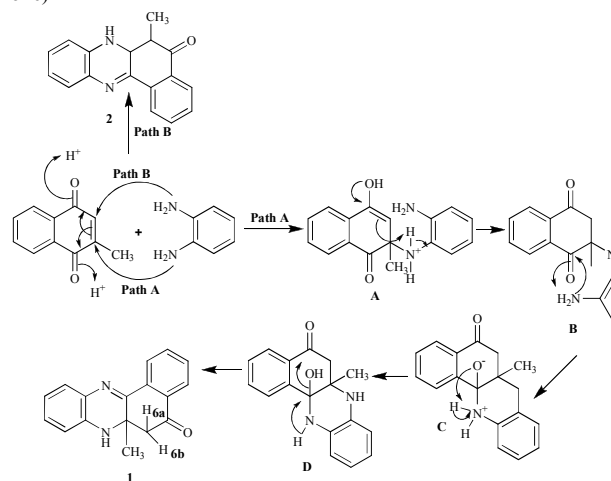
The dihydrobenzophenazine (DHBP) derivatives, nitrogen containing heterocyclic compounds, have attracted significant attention in the recent years owing to their potential applications as antibacterial¹, antimalarial², antituberculosis³ properties in pharmaceutical chemistry. DHBP derivative are comprised of planar aromatic polycyclic structure rendered with topoisomerase I and II enzyme inhibitor^{4,5} activities which facilitates their use as the potential anticancer target. The vital role of DHBP derivative in the field of medicine has provided impetus to undertake this study.⁶ We herewith report the synthesis and characterization of 6a-methyl-6a,7-dihydrobenzo[α]phenazin-5(6H)-one; **1** using precursor vitamin K3 displayed in Scheme 1.

It has been pointed out in the literature that the synthesis of DHBP derivatives were carried out by the reaction of naphthol¹, 1,2-naphthoquinone¹, lawsone⁷, laphocol^{8,9} with *o*-phenylenediamine, electrochemical¹⁰ and green chemistry approach.¹¹ In the present endeavor, sulfuric acid was used to catalyze the Michael addition followed by condensation of *o*-phenylenediamine with vitamin K3, (2-methyl-1,4-naphthoquinone). The DHBP derivative **1** thus obtained was thoroughly characterized by single crystal X-ray diffraction, FT-IR, UV-visible, ¹H,¹³C-NMR, 2D-NMR, LC-MS experiments. To envisage the conformational characteristics we performed the calculations based on density functional theory.

Experiments have shown that the formation of product 6a-methyl-6a,7-dihydrobenzo[α]phenazin-5(6H)-one (**1**) is preferred (Path A) over **2** shown in the path B of Scheme 2.



Scheme 1 Molecular structures of vitamin K3(2-methyl-1 naphthoquinone) and **1**(6a-methyl-6a,7-dihydrobenzo[α]phenazin-5(6 one)



Scheme 2 Plausible mechanism for formation of 6a-methyl-6a dihydrobenzo[α]phenazin-5(6H)-one (**1**)

As shown in the Scheme 2 the protonation of the carbonyl group at C(4) position of α, β -unsaturated system in vitamin K3 favours the formation of nearly stable carbocation bound to methyl group, which influences the Michael addition of nucleophile to amino group at C(2) position of *o*-phenylenediamine thereby generating the intermediate species 'A' (Scheme 2). More often nucleophile addition prefer sterically less demanding approach to attack on Michael acceptor and hence it may be expected to give

Department of Chemistry, Savitribai Phule Pune University, Pune 411007, India;
Fax: +912025693981; Tel: +912025601397 -Ext-531; E-mail:
sunitas@chem.unipune.ac.in

Department of Chemistry, Indian Institute of Technology, Ropar, Rupnagar-140001,
Punjab, India

† Electronic Supplementary Information (ESI) available: Fig.S1LC-MS spectrum, Fig.S2-Fig.S-4 FT-IR figures, Fig.S5 DSC spectrum, Fig.S6-Fig.S8 NMR, Fig.S9 UV-visible spectra, Fig.S10 HOMO-LUMO diagram, Fig. S11 Optimized IR spectra, Table 1 and Table 2 Crystallography data. See DOI: 10.1039/x0xx00000x

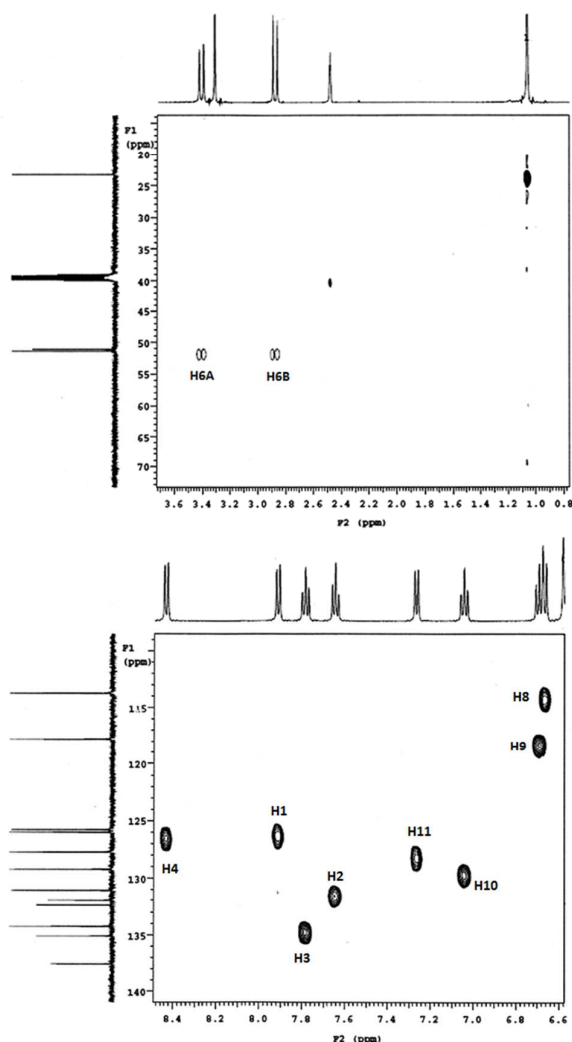


Fig.1 gHSQC NMR spectra of **1**

product **2** preferentially. On the contrary we observed the protonation favours the formation of product **1**. Furthermore, protonation of the resulting enol in intermediate species **A** occurs subsequent to loss of hydrogen from the positively charged nitrogen species yielding the neutral species 'B'. The other amino functionality in *o*-phenylenediamine orient itself closer enough to attack on the C(1) carbon of the carbonyl group in vitamin K3. Thus resulting condensation generates the C-N bond as indicated by intermediate 'C'. The proton transfer facilitates the formation unstable aminol functionality (species D) subsequently loses water molecule yielding **1**. The mass spectroscopic analysis of DHBPI showed the presence of relatively intense M+1 molecular ion peak at m/z 263 (Fig.S1 in ESI[†]). Its FT-IR spectroscopic analysis has indicative of a band at 3300 cm^{-1} (Fig.S3 in ESI[†]) assigned to $\nu_{\text{N-H}}$ stretching of the free -N-H moiety in DHBPI derivative **1**. The other intense FT-IR bands appeared at 1601 cm^{-1} and $\sim 1298\text{ cm}^{-1}$ were

Table 1 Hydrogen bond geometries for **1**

D-H...A	D-H(Å)	H...A(Å)	D...A(Å)	\angle D-H...A(°)
N(7)-H(7A)...O(1) ⁽ⁱ⁾	0.90(2)	2.12 (2)	3.027(2)	176(1)
C(6)-H(6B)...C(9) ⁽ⁱⁱⁱ⁾	0.969(1)	2.830(2)	3.720(2)	153.0(1)
C(1)-H(1)...C(2) ⁽ⁱⁱⁱ⁾	0.930(1)	2.817(2)	3.621(2)	145.4(1)

(i) -1/2+x, 1/2-y, 1-z (ii) -1+x,y,z (iii) -1/2+x,y,1.5-z

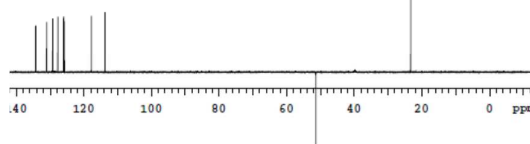


Fig.2 DEPT NMR spectra of **1**

assigned to carbonyl (C(5)) and imino (C(12A)) stretching of the paranaphthoiminoquinone moiety, respectively.

The sharp singlet at $\delta = 1.06$ in the measured ^1H NMR spectrum (Fig.S6 in ESI[†]) in $\text{DMSO-}d_6$ of **1** attributed to the methyl group attached to C(13). Moreover, the spectrum showed the characteristic geminal coupling pattern corresponding to non-equivalent methylene protons H(6A) and H(6B) which concomitantly emerge as a doublet of doublet at $\sim \delta = 2.8$ and 3.4 respectively. The differences in chemical shifts between these two protons could be explained as per the conformation observed in the X-ray single crystal of DHBPI derivative **1**. The H(6A) proton has been appearing at slightly upfield than H(6B) proton; since it has been found to present in the shielding zone of the aromatic nucleus, whereas H(6B) proton has been seen away from shielding zone of the aromatic nucleus and in addition to that H(6B) proton also coming under the influence of deshielding zone of the adjacent carbonyl group at C(5) position. Thus overall effect on H(6B) proton indicative of the distinct downfield chemical shift at $\delta = 3.4$. Normally, $\text{CH}_3\text{-O}$ appears at this chemical shift in the ^1H NMR spectrum; the formation of product **1** is thus evident. The product **2** (Path B, Scheme 2) is expected to emerge with distinct pattern in its ^1H NMR spectrum.

The Heteronuclear Single Quantum Coherence (gHSQC) experiments further revealed peaks (Fig.1) confirm the presence of nonequivalent C(6) methylene protons and aliphatic carbon and its attached proton are correlated. As a result gHSQC study also supports to get the complete information related to structure of the DHBPI derivative **1**. The DEPT NMR experiment gives an idea about presence of CH_3 (C(13)), CH (aromatic), CH_2 (C(6), α -carbon) groups and quaternary carbon (C(6A)) (Fig.2). Accordingly, we notice the normal ^{13}C peak for CH_3 and CH carbons; the peak for the quaternary carbon (C(6A)) disappears. The presence of inverted peak assigned to methylene at C(6) are supports the inference of regioselective addition of the *o*-phenylenediamine.

The UV-Visible spectrum (Fig.S9 in ESI[†]) of the DHBPI derivative **1** showed a broad band at $\sim 264\text{-}273\text{ nm}$, indicative of the presence of $\text{C}=\text{N}$ at C(12A) as well as aromatic rings. The appearance of UV band near 311 nm results from $\pi\text{-}\pi^*$ transition of the $\text{C}=\text{O}$ functionality.¹²

The single crystal X-ray diffraction of DHBPI derivative **1** shows the crystallization in orthorhombic space group *Pbca* which contains eight molecules in unit cell. Fig.3 showed an ORTEP plot. Single crystal X-ray structure underlines the regioselective addition of *o*-phenylenediamine at C(2) and the condensation with carbonyl group present at C(1) of the vitamin K3. The carbonyl bond distance (C(5)-O(1)) was 1.21 \AA which is similar to that observed in oxidized form of naphthoquinone carbonyls.¹³ The sp^3 hybridization of carbon atoms C(6) and C(6A) was thus inferred from the bond distance parameters *viz* C(6)-C(6A); 1.519 \AA , C(6A)-C(12A); 1.522 \AA and C(6)-C(5); 1.494 \AA . Thus, N(7) and N(12) atom centers are suggested to be sp^3 and sp^2 hybridized, respectively.¹⁴

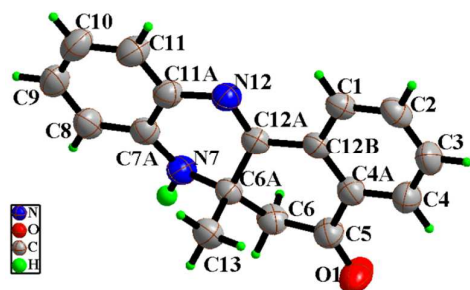


Fig.3 ORTEP plot of **1**. CCDC number 973251, Formula: $C_{17}H_{14}N_2O$, Formula weight: 262.30, Orthorhombic crystal system, space group: $Pbca$, $a/\text{\AA} = 7.518(5)$, $b/\text{\AA} = 14.238(5)$, $c/\text{\AA} = 25.049(5)$, $V(\text{\AA}^3) = 2681(2)$, $Z = 8$, $R1 = 0.0363$. Bond distances: $C(5)-O(1) = 1.217(2)$, $C(5)-C(6) = 1.492(2)$, $C(6)-C(6A) = 1.519(2)$, $C(6A)-C(12A) = 1.521(2)$, $C(6A)-C(7) = 1.453(2)$, $N(7)-C(7A) = 1.375(2)$, $N(12)-C(11A) = 1.285(2)$, $N(12)-C(12A) = 1.405(2)$. $\angle N(7)-C(6A)-C(6) = 112.3(1)$, $\angle C(5)-C(6)-C(6A) = 114.0(1)$

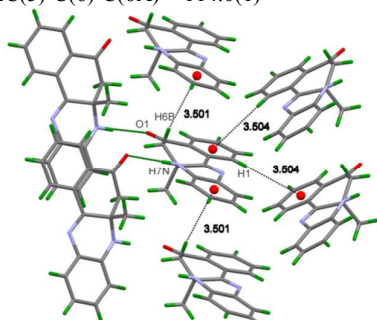


Fig.4 C-H... π and N-H...O interactions of (**1**)

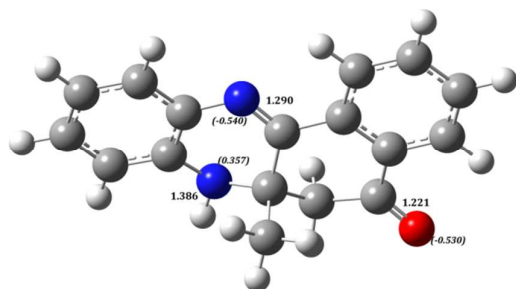


Fig.5 B3LYP/6-31+G(d,p) optimized structure of (**1**). Selected bond distance parameters (in \AA) and Hirshfeld atomic charges (given in parentheses) are shown

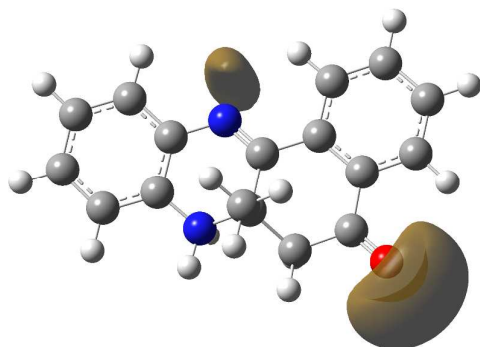


Fig.6 Molecular electrostatic potential surface of **1** (isosurface $V = -52.5 \text{ kJ mol}^{-1}$)

The wire frame diagram of DHBP derivative **1** showed the presence of C-H... π interactions between the two aromatic rings A and D (Scheme 1) of the neighboring molecules. It help to facilitate the crystal network (Fig.4), wherein the molecules from neighboring polymeric chain combine in *head to head* fashion revealing N-H...O interactions. The hydrogen bonding structural parameters are reported in Table 1.

The molecular structure of DHBP derivative **1** was optimized within the framework of density functional theory incorporating the B3LYP P(Becke, Lee-Yang-Parr 3 parameter exchange correlation functional)^{15,16} (*cf.* Fig.5) employing the Gaussian-09 program.¹⁷ The internally stored basis with diffuse functions being added on all the heavy atoms, designated with the 6-31+G(d,p) basis, was used. Stationary point structure thus obtained was confirmed to be local minimum on the potential energy surface through vibrational frequency calculations. Net atomic charges have been derived from population analysis based on the Hirshfeld partitioning scheme. The electron-rich regions of DHBP derivative **1** have further been characterized in terms of molecular electrostatic potential (MESP) which are portrayed in Figure 6. Normal vibrations were assigned by visualizing displacements of atoms about their equilibrium (mean) positions combined with the potential energy distribution. The vibrational frequencies from the present DFT calculations are scaled by a factor of 0.9654; obtained from a comparison with the carbonyl stretching frequency in the measured spectra (1674 cm^{-1}). The highest wave number vibration was assigned to -NH stretching appears at 3458 cm^{-1} which corresponds to (observed: 3300 cm^{-1}) band in the experiment. Likewise the aromatic -CH stretching appear at the 3115 cm^{-1} , 3106 cm^{-1} and 3060 cm^{-1} , respectively (observed: 3051 cm^{-1}), whereas the methylene stretching corresponds to the 2988 cm^{-1} . The methyl vibrations appear $\sim 3015 \text{ cm}^{-1} - 2929 \text{ cm}^{-1}$ (the lowest vibration arising from the locally symmetric -CH₃ functionality). The experimental spectra revealed aromatic -CH and the methylene stretching in the region (observed: $2959, 2918 \text{ cm}^{-1}$). Overall the calculated IR spectra are in fairly good agreement with those in the IR spectra.

The DHBP derivative **1** with both chair and boat conformers were optimized within the framework of density functional theory. The chair and boat forms of the isolated DHBP derivative **1** finally converged to the one structure portrayed in Fig.5. Selected bond distance parameters (in \AA) and Hirshfeld atomic charges (in parentheses) are depicted in Fig.5. Structural parameters from the present theory are in consonant with those from the single crystal X-ray data reported in Table S2 of the supporting information. MESP analyses have shown that the electron-rich regions by and large, are localized near carbonyl oxygen and pyridinium nitrogen. It may, therefore, be inferred that crystal network extends *via* N-H...O interactions. MESP isosurface ($V = -52.5 \text{ kJ mol}^{-1}$) has been depicted in Fig.6. The highest occupied molecular orbital (isosurface of $-17.5 \text{ kJ mol}^{-1}$) in the DHBP derivative **1** has been shown in Fig.S10 in the supporting information.

To summarize, a regioselective synthesis of 6a-methyl-6a,7-dihydrobenzo[α]phenazin-5(6H)-one *i.e.* dihydrobenzophenazine derivative **1** based on vitamin K3 has been reported in the present work. The regioselective yield of the product has been confirmed from the single crystal X-ray diffraction data and further supported by its electronic structure derived from the B3LYP/6-31+G(d,p) theory. The studies on reactions of 1,4-naphthoquinone derivatives with *o*-phenylenediamine are in progress in our laboratory.

SSG is grateful the Department of Biotechnology, India for the financial support. DC thanks the University Grants Commission, New Delhi, India for the Junior Research Fellowship. SSR acknowledges the financial support from the Savitribai Phule Pune

University, Pune, India for the award of research fellowship through the potential excellence scheme.

† Notes and references

Analytical data of **1**, Color: Dark orange, Yield: 0.459 g (30.13%), M.P. 152.27°C. FT-IR (KBr; cm^{-1}): 3300, 3051, 2959, 2918, 1674, 1600, 1477, 1450, 1427, 1365, 1338, 1298, 1263, 1209, 1167, 1108, 1076, 1057, 1026, 987, 943, 893, 873, 815, 795, 731, 680, 644, 586, 567, 594, 488, 432. ^1H NMR (500 MHz), $\delta(\text{ppm})$: 1.06(3H, s), 2.84 (1H, d, $J = 15.50$ Hz), 3.40 (1H, d, $J = 15.50$ Hz), 6.67 (1H, d, $J = 8.00$ Hz), 6.69 (1H, d, $J = 8.25$ Hz), 7.04 (1H, d, $J = 8.25$ Hz), 7.25 (1H, d, $J = 8.00$ Hz), 7.64 (1H, d, $J = 7.50$ Hz), 7.78 (1H, d, $J = 8.25$ Hz), 7.90 (1H, d, $J = 8.00$ Hz), 8.43 (1H, d, $J = 8.00$ Hz), ^{13}C NMR (125 MHz DMSO- d_6), $\delta(\text{ppm})$: C(1) = 125.79, C(2) = 131.05, C(3) = 134.28, C(4) = 126.01, C(4a) = 132.42, C(5) = 194.60, C(6) = 51.37, C(7) = 51.08, C(7A) = 132.12, C(8) = 113.78, C(9) = 117.79, C(10) = 129.26, C(11) = 127.74, C(11A) = 137.57, C(12A) = 155.80, C(12B) = 131.99. UV-Vis; DMSO (λ_{max} , nm): 437, 317, 271, 262. Anal. data. Calc. for $\text{C}_{17}\text{H}_{14}\text{N}_2\text{O}$: C, 77.84; H, 5.38, N, 10.68, Found: C, 77.34; H, 5.40, 11.16.

- H. Hussain, S. Specht, S. R. Sarite, M. Saeftel, A. Hoerauf, B. Schulz, and K. Krohn, *J. Med. Chem.*, 2011, **54**, 4913-4917.
- M. E. Makgatho, R. Anderson, J. F. O'Sullivan, T. J. Egan, J. A. Freese, N. Cornelius and C. E. J. Van Rensburg, *Drug Dev. Res.*, 2000, **50**, 195-202.
- R. S. F. Silva, M. C. F. R. Pinto, M. O. F. Goulart, J. D. S. Filho, I. Neves Jr, M. C. S. Lourenco and A. V. Pinto, *Eur. J. Med. Chem.*, 2009, **44**, 2334-2337.
- S. -T. Zhuo, C. -Y. Li, M. -H. Hu, S. -B. Chen, P. -F. Yao, S. -L. Huang, T. -M. Ou, J. -H. Tan, L. -K. An, D. Li, L. -Q. Gu and Z. -S. Huang, *Org. Biomol. Chem.*, 2013, **11**, 3989-4005.
- N. Vicker, L. Burgess, I. S. Chuckowree, R. Dodd, A. J. Folkes, D. J. Hardick, T. C. Hancox, W. Miller, J. Milton, S. Sohal, S. Wang, S. P. Wren, P. A. Charlton, W. Dangerfield, C. Liddle, P. Mistry, A. J. Stewart and W. A. Denny, *J. Med. Chem.*, 2002, **45**, 721-739.
- D. Chadar, S. S. Rao, A. Khan S. P. Gejji, K. S. Bhat, T. Weyhermüller and S. Salunke-Gawali, *RSC Adv.*, 2015, **5**, 57917-57929.
- B. -L. Yao, Y. -W. Mai, S. -B. Chen, H. -T. Xie, P. -F. Yao, T. -M. Ou, J. -H. Tan, H. -G. Wang, D. Li, S. -L. Huang, L. -Q. Gu and Z. -S. Huang, *Eur. J. Med. Chem.*, 2015, **92**, 540-553.
- P. F. Carneiro, M. C. F. R. Pinto, T. S. Coelho, B. C. Cavalcanti, C. Pessoa, C. A. Simone, I. K. C. Nunes, N. M. de Oliveira, R. G. de Almeida, A. V. Pinto, K. C. G. de Moura, P. A. da Silva and E. N. da Silva Júnior, *Eur. J. Med. Chem.*, 2011, **46**, 4521-4529S.
- M. J. da Silva, M. C. F. R. Pinto, C. A. de Simone, J. G. Soares, J. R. M. Reys, J. D. de S. Filho, W. T. A. Harrison, C. E. M. Carvalho, M. O. F. Goulart, E. N. da Silva Júnior and A. V. Pinto, *Tetrahedron Lett.*, 2011, **52**, 2415-2418.
- S. S. H. Davarani, A. R. Fakhari, A. Shaabani, H. Ahmar, A. Maleki and N. S. Fumani, *Tetrahedron Lett.*, 2008, **49**, 5622-5624.
- A. C. Sousa, M. C. Oliveira, L. O. Martins and M. Pa. Robalo, *Green Chem.*, 2014, **16**, 4127-4136.
- D. Chadar, M. Camilles, R. Patil, A. Khan, T. Weyhermüller and S. Salunke-Gawali, *J. Mol. Struct.*, 2015, **1086**, 179-189.
- (a) R. Patil, D. Chadar, D. Chaudhari, J. Peter, M. Nikalje, T. Weyhermüller and S. Salunke-Gawali, *J. Mol. Struct.*, 2014, **1075**, 345-351. (b) S. Pal, M. Jadhav, T. Weyhermüller, Y. Patil, M. Nethaji, U. Kasabe, L. Kathawate, V. B. Konkimalla and S. Salunke-Gawali, *J. Mol. Struct.*, 2013, **1049**, 355-361. (c) O. Pawar, A. Patekar, A. Khan, L. Kathawate, S. Haram, G. Markad, V. Puranik and S. Salunke-Gawali, *J. Mol. Struct.*, 2014, **105**, 68-74. (d) S. Salunke-Gawali, O. Pawar, M. Nikalje, R. Patil, T. Weyhermüller, V. G. Puranik and V. B. Konkimalla, *J. Mol. Structure.*, 2014, **1056-1057**, 97-103.
- L. Kathwate, P. V. Joshi, T. Dash, S. Pal, M. Nikalje, T. Weyhermüller, V. G. Puranik, V. B. Konkimalla and S. Salunke-Gawali, *J. Mol. Struct.*, 2014, **1075**, 397-405.
- Frisch, M. J. Trucks, G. W. Schlegel, H. B. Scuseria, G. E. Robb, M. A. Cheeseman, J. R. Montgomery, J. A., Jr. Vreven, T. Kudin, K. N. Burant, J. C. Millam, J. M. Iyengar, S. S. Tomasi, J. Barone, V. Mennucci, B. Cossi, M. Scalmani, G. Rega, N. Petersson, G. A. Nakatsuji, H. Hada, M. Ehara, M. Toyota, K. Fukuda, R. Hasegawa, J. Ishida, M. akajima, T. Honda, Y. Kitao, O. Nakai, H. Klene, M. Li, X. Knox, J. E. Hratchian, H. P. Cross, J. B. Bakken, V. Adamo, C. Jaramillo, J. Gomperts, R. Stratmann, R. E. Yazyev, O. Austin, A. J. Cammi, R. Pomelli, C. Ochterski, J. W. Ayala, P. Y. Morokuma, K. Voth, G. A. Salvador, P. Dannenberg, J. J. Zakrzewski, V. G. Dapprich, S. Daniels, A. D. Strain, M. C. Farkas, O. Malick, D. K. Rabuck, A. D. Raghavachari, K. Foresman, J. B. Ortiz, J. V. Cui, Q. Baboul, A. G. Clifford, S. Cioslowski, J. Stefanov, B. B. Liu, G. Liashenko, A. Piskorz, P. Komaromi, I. Martin, R. L. Fox, D. J. Keith, T. Al-Laham, M. A. Peng, C. Y. Nanayakkara, A. Challacombe, M. Gill, P. M. W. Johnson, B. Chen, W. Wong, M. W. Gonzalez, C. Pople and J. A. Gaussian03, revision Gaussian, Inc.: Pittsburgh, PA, 2003.
- D. J. Becke, *Chem. Phys.*, 1993, **98**, 5648-5652.
- C. Lee, W. Yang and R. G. Parr, *Phys. Rev.*, 1988, **B37**, 785-789.